

How moderate sea states can generate loud seismic noise in the deep ocean

M. J. Obrebski,¹ F. Ardhuin,¹ E. Stutzmann,² and M. Schimmel³

Received 2 April 2012; revised 27 April 2012; accepted 27 April 2012; published 1 June 2012.

[1] The location of oceanic sources of the micrometric ground displacement recorded at land stations in the 0.1–0.3 Hz frequency band (“double frequency microseisms”) is still poorly known. Here we use one particularly strong noise event in the Pacific to show that small swells from two distant storms can be a strong deep-water source of seismic noise, dominating temporarily the signals recorded at coastal seismic stations. Our interpretation is based on the analysis of noise polarization recorded all around the source, and the good fit achieved for this event and year-round between observed and modeled seismic data. The model further suggests that this is a typical source of these infrequent loud noise bursts, which supports previous inconclusive evidences of the importance of such sources. This new knowledge based on both modeling and observations will expand today’s limits on the use of noise for climate studies and seismic imaging. **Citation:** Obrebski, M. J., F. Ardhuin, E. Stutzmann, and M. Schimmel (2012), How moderate sea states can generate loud seismic noise in the deep ocean, *Geophys. Res. Lett.*, 39, L11601, doi:10.1029/2012GL051896.

1. Introduction

[2] Between earthquakes, seismic stations record a background of ground motion. With a typical vertical displacement of the order of a few microns, these tremors are generally referred to as “microseisms”. The link between seismic noise and ocean wave activity has been progressively established over the past 140 years [Algué, 1900; Bernard, 1990]. Therefore, just as buoy observations, seismic noise provides a measure of the frequency content of ocean waves, although seismic stations sample wave-induced noise from a broader area. Seismic stations are comparatively more widespread over the Globe, and they provide records that generally predate those from buoys and satellites. Because of these advantages, seismic noise has been used to characterize sea states and their relation to possible climate changes over the 20th century [Bernard, 1981; Bromirski et al., 1999; Grevemeyer et al., 2000; Aster et al., 2008; Stutzmann et al., 2009]. Compared to earthquakes, seismic noise is recorded continuously and has thus great potential for seismic monitoring [Shapiro et al., 2005; Brenguier et al., 2008; Zhang et al., 2010a]. In its current state, the analysis of

seismic noise provides important constraints on trends in oceanic storminess and the Earth internal structure. Nevertheless, the exact location of microseismic sources in time, space and frequency is still poorly known, and we could enhance the accuracy and reach of noise-based analysis if we could track these sources [Tsai, 2009].

[3] The physical processes responsible for seismic noise generation in the ocean are understood since the mid-XXth century. Wave transformation in very shallow water is responsible for a modest peak of noise in the frequency band 0.05–0.1 Hz (“primary microseisms”) while non-linear interactions between oppositely traveling waves with similar frequencies induce pressure fluctuation of wavelengths much larger than that of ocean waves, and thus capable of driving seismic waves [Miche, 1944; Longuet-Higgins, 1950; Hasselmann, 1963]. The body- and surface-waves excited through this mechanism have frequencies that are twice that of the interacting ocean waves and are thus referred to as “double frequency microseisms” (DFM hereafter), with strongest energy in the band 0.1–0.2 Hz.

[4] Based on numerical simulation, it was found [Ardhuin et al., 2011] that DFM sources exist within any storm, with a strength that varies by several orders of magnitude of the dominant waves due to the varying width of the directional distribution of wave energy. Higher noise levels are usually recorded when waves are reflected from shorelines, and numerical models [Ardhuin et al., 2011] suggest that the loudest of all noise sources occur where waves running away from a storm as swell meet another swell or a wind sea, and that this situation may explain most of the recorded noise at mid-ocean islands. Compressional body-waves (P) have been unambiguously associated to deep ocean sources induced by large storms such as the 2006 typhoon Ioke [Haubrich and McCamy, 1969; Zhang et al., 2010b]. Surface-wave polarization analysis using several arrays or individual stations [Cessaro, 1994; Chevrot et al., 2007; Stutzmann et al., 2009] gave strong indications that DFM sources in the deep ocean also produce Rayleigh waves recordable at continental stations several thousands of kilometers away. Yet, as illustrated by a recent review [Bromirski, 2009], this last point is still debated. The main reason is that surface-wave analysis does not allow resolving the station-to-source distance, and it is thus difficult to rule out that multiple sources could be distributed along the estimated station-to-source azimuth, in particular near the coast. To remove this ambiguity, a recent study [Kedar et al., 2008] combined surface wave polarization analysis and a wave model to map all possible sources during a presumably deep-ocean seismic noise burst, also detected using microseismic body waves analysis [Landès et al. 2010]. Although Kedar et al.’s numerical approach satisfies the data, their wave model does not account for coastal reflection and thus it cannot guarantee

¹Laboratoire d’Océanographie Spatiale, Ifremer, Plouzané, France.

²IPGP, PRES Université Paris-Cité, Paris, France.

³Institute of Earth Sciences Jaume Almera, CSIC, Barcelona, Spain.

Corresponding author: M. J. Obrebski, Laboratoire d’Océanographie Spatiale, Ifremer, BP 70, F-29280 Plouzané CEDEX, France. (mathias.obrebski@ifremer.fr)

Copyright 2012 by the American Geophysical Union.
0094-8276/12/2012GL051896

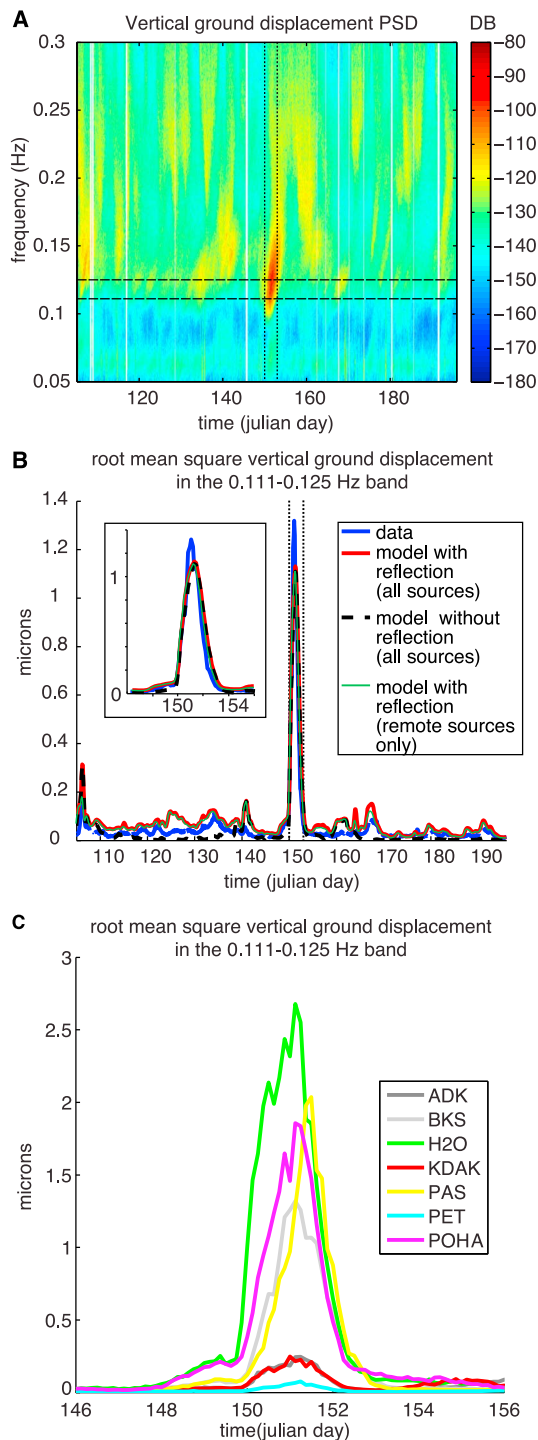


Figure 1. Seismic noise recorded from April 15th to July 15th at BKS. A burst is observed on May 30th–31st (Julian days 150–151) in the (a) frequency and (b) time domains. The peak is well modeled with (red line) or without (black dashed line) computation of the ocean waves reflection on the coast, suggesting little effect of the later. The green line was computed without the contribution of the closest sources, within 330 km from BKS (see location on Figure 3), and shows that the 95% of the ground motion results from remote sources. (c) The May 2002 burst of seismic noise as recorded by land-, island- and ocean bottom-based stations located all around the East Pacific Basin. The location of stations is displayed on Figure 2.

that the later did not noticeably contributed to the noise generation. Extending previous data-based and numerical approaches, our double objective here is to show that loud and recordable DFM sources of Rayleigh waves exist in the deep ocean, and to show how they relate to sea states.

2. Data and Method

[5] To locate DFM sources in time and space, we perform a polarization analysis [Schimmel and Gallart, 2004; Schimmel et al. 2011] (see Text S1 in the auxiliary material) at individual stations to estimate the azimuth to the noise source (back-azimuth).¹ We analyze anomalously high noise episodes recorded simultaneously by several individual seismic stations, and we triangulate the back-azimuths to constrain the source location. This analysis is combined with a numerical wave model [Tolman, 2008; Arduin et al. 2010] modified to compute and map seismic sources. In addition to validating the location of the source region estimated through back-azimuths triangulation, the wave model allows checking that the source region is unique. Compared to earlier wave models [Kedar et al., 2008], we take into account the possibly important contribution of coastal reflections. A comprehensive description of the methods is given in the auxiliary material. We focus on the Eastern Pacific Basin because large storms are frequent there, and because it is wide enough to unambiguously find sources far from any coast. This part of the Globe is also well covered in terms of continent- and island-based seismic stations. This includes the seismic stations ADK (Adak, Alaska), KDAK (Kodiak, Alaska), H2O (Hawaii-2 Observatory, USA), PAS (Pasadena, California), POHA (Pohakuloa Training Area, Hawaii) and PET (Petropavlovsk-Kamchatskiy, Russia). We primarily analyze years 2002–2003, in order to benefit from the dataset of the ocean bottom station Hawaii-2 Observatory (H2O).

3. Results

3.1. Observed and Modeled Time Series During the May 2002 Noise Burst

[6] We detect several microseismic bursts that are consistent with deep-ocean sources. Here we describe the most energetic event, recorded from May 29th, 2002 (Julian day 149) to June 1st (day 152). Figure 1 shows the corresponding frequency-time diagram of the vertical ground motion (median over 3 hours) recorded by the Berkeley seismic station (BKS, California). Figure 1b also illustrates the good agreement between observed and synthetic root mean square vertical ground displacements (RMSVGD), which validates our numerical model. The RMSVGD amplitude is slightly underestimated during the burst. This can result from the spatially uniform quality factor Q assumed in our model (see Text S1 in the auxiliary material), and small errors in the numerical wave model. Of particular interest, the synthetics are almost identical, whether coastal reflection is taken into account or not (see also Figure S1). This indicates that coastal reflection is not necessary to explain the recorded signal during that event, although it is necessary to reproduce the variability of the signal throughout the year (compare to days

¹Auxiliary materials are available in the HTML. doi:10.1029/2012GL051896.

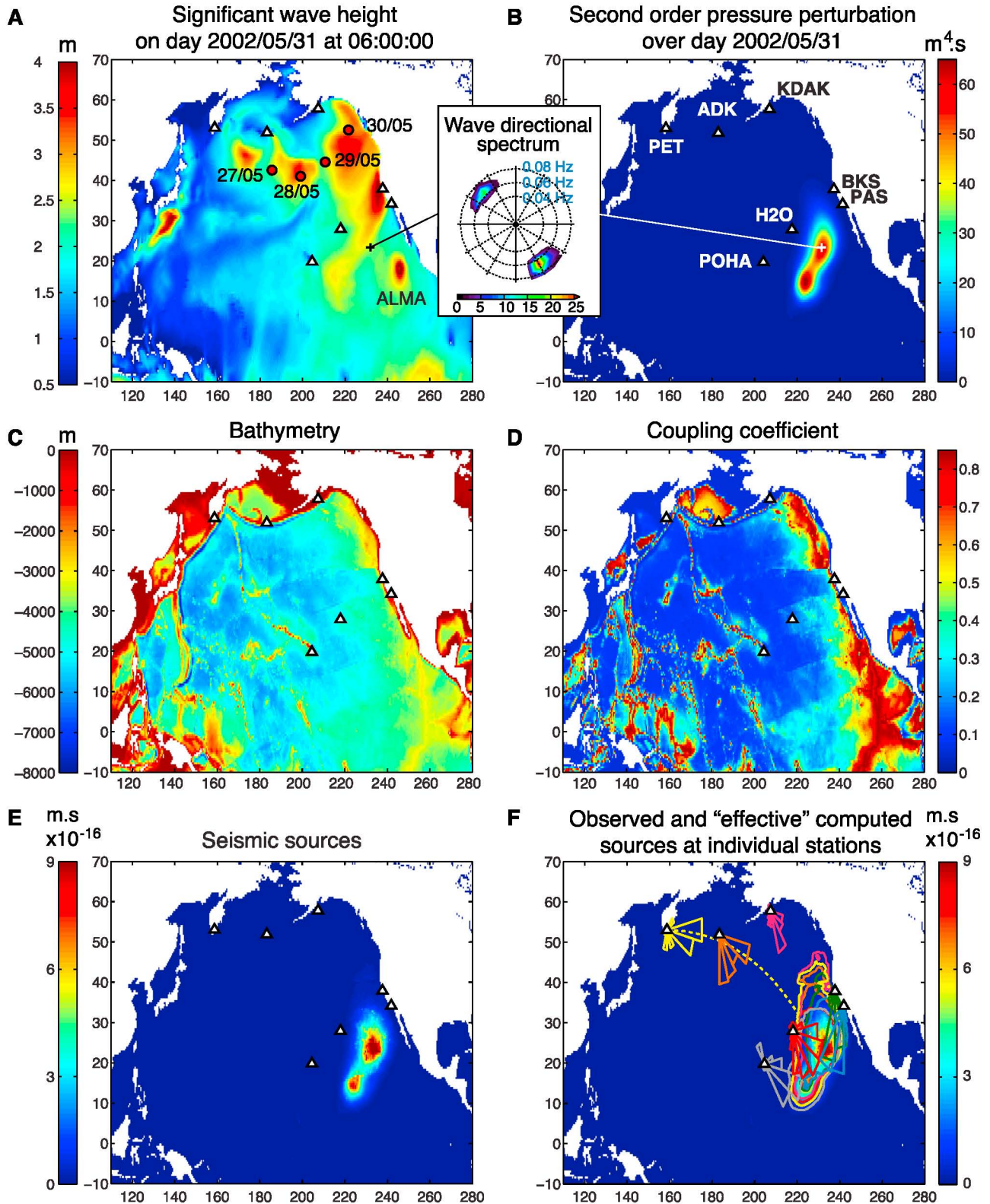


Figure 2. Generation of the May 2002 seismic noise burst. (a) An extra-tropical storm (track indicated by red dots) and hurricane “Alma” produce swells with nearly opposite direction where (b) the wave induced pressure perturbation is maximum. (c) The bathymetry governs (d) the amplification factor between the surface pressure and (e) the modeled sources of Rayleigh waves. (f) The observed azimuthal distribution of incoming Rayleigh waves estimated by polarization analysis. All dominant polarizations point toward a single region, where the computed “effective” sources (bound by colored 90% contours) are concentrated and largely overlap. The yellow dotted line indicates the great circle traced from PET in the observed dominant direction.

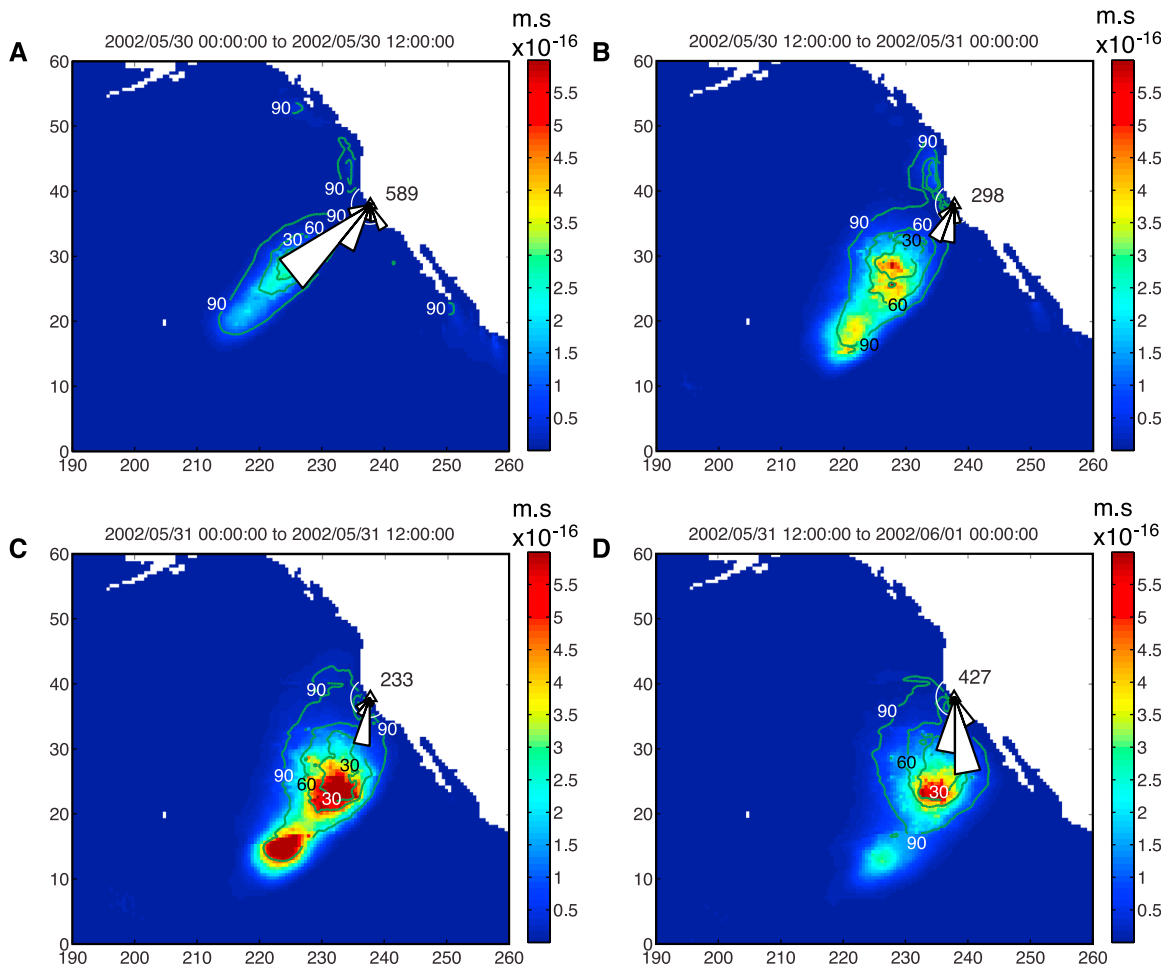


Figure 3. Migration of the “effective” noise sources for station BKS. (a–d) The azimuthal distribution of incoming Rayleigh waves and total number of polarized noise samples estimated by polarization analysis over half day-long time slots. The background images show all the computed seismic sources (as on Figure 2e), while the contours bound 90, 60 and 30% of the “effective” sources that specifically contribute to the ground displacement at BKS. The white arc around BKS has 330 km radius. The observed dominant direction undergoes an anti-clockwise rotation, in consistency with the southeastward migration of the computed sources.

110–140 on Figure 1b when the model without reflection does not satisfy the data). Besides, computations indicate that 95% of the RMSVGD is due to remote sources (Figure 1b). Several stations (Figure 1c) located all around the Eastern Pacific Basin (Figure 2), also recorded this event. In each case, the agreement between observed and synthetic RMSVGD is good and the wave model indicates that reflection at the coast is not involved in the excitation of microseismic sources (Figure S2). The RMSVGD measured by land stations in the narrow 0.114–0.125 Hz band ranges from 0.08 microns at PET to 2 microns at PAS, and it reaches 2.5 microns at the ocean bottom stations H20, which is the highest recorded value in its 1.5-years long deployment.

3.2. Relation to Sea-States

[7] The wave model shows how this exceptional noise event is associated to the encounter, unusual for such long-period waves, of two swells traveling exactly in opposite directions (Figure 2). These numerical results are robust as indicated by the good match with satellite and buoy wave measurements (Figure S4). An extra-tropical storm that followed the usual north-Pacific storm track peaked earlier on

May 27th with wave heights up to 10 m, and radiated the broad band of 2.5–3 m high swell that extends from BKS to the south-east of POHA. This swell interacts with another swell from hurricane “Alma” (category III), which is still active west of Mexico. Where these swells encounter each other, their non-linear interactions induce a pressure perturbation [Longuet-Higgins, 1950] at the sea surface that contains the very long wavelength oscillations capable of driving seismic waves (Figure 2b). The bathymetry (Figure 2c) determines the amplification coefficient (Figure 2d) that multiplies the surface pressure to give the local seismic source (Figure 2e). According to our wave model, the power of DFM sources described here is not among the strongest documented events. In particular, it is 140 times less than during the 1998 DFM burst in the Labrador sea [Schulte-Pelkum *et al.*, 2004] (Figure S5) induced by stronger waves (up to 14 m) and enhanced by the locally large coupling coefficient associated with shallower ocean depth. Nevertheless, our noise event is particularly interesting because its strongest DFM sources (Figures 2e and 2f) coincide with a region of very moderate wave height, only around 2.5 m (Figure 2a), and located far in space and time from the two

storms that generated the swells. This illustrates the caution required when using seismic noise observations as an indirect method to estimate wave heights and climate proxies: A loud noise event does not imply a locally intense sea state, and the noise maximum does not necessarily match that of wave height.

3.3. Noise Polarization Analysis

[8] The location of sources estimated by analyzing the polarization of noise recorded on May 30th–31st coincides with that obtained numerically, which further validates our numerical approach (Figure 2f). The polarization analysis provides constraints on the direction to the source (“back azimuth”) of Rayleigh waves contained in noise records. All back-azimuths estimated at each station during May 31st are compiled in angular histograms and displayed on Figure 2f. The main directions observed at individual stations all converge toward the computed sources. The RMSVGD at a given station integrates the contribution of all sources (Figure 2e), taking into account along-path energy decay resulting from geometrical spreading and inelasticity. Figure 2f also shows these “effective” sources sorted and contoured. During the microseismic burst, they are concentrated in single contours that largely overlap. By contrast, the effective sources are diffuse before and after the burst (Figure S6). The most energetic sources are centered at 125°W/23°N on day 151 (Figure 2e), i.e., 1770 km from H2O, and 7100 km from PET. These two stations record respectively the highest and lowest levels of noise, consistent with their respective distance to the sources.

3.4. Size and Motion of the Source Region

[9] Figure 3 shows the evolution of the back-azimuth histograms and computed sources on a 12 hours-long basis at station BKS from May 30th to May 31st. The modeled sources gradually migrate to the southeast and this motion corresponds to the anticlockwise rotation observed in the back-azimuth histograms. On the first half of May 31st, at the climax of the microseismic burst, the regions that contain 30, 60 and 90% of the strongest effective sources have areas of 1150 by 500 km, 1500 by 1000 km and 3000 by 1650 km, respectively. Surprisingly, this is when the number of polarized noise samples is the lowest. At this particular moment, the source is the widest. Station BKS samples simultaneously surface waves from multiple back-azimuths, degrading the efficiency of the polarization analysis. This detailed analysis of the wave model, validated by the polarization analysis, shows that microseismic bursts can undergo noticeable variations in width, intensity and location.

4. Conclusions and Perspectives

[10] The noise event specifically described here shows how moderate waves from distant storms, with the right combination of energy in opposite directions, can induce a very loud noise. A second important result is that deep-ocean microseismic sources exist in the middle of ocean basins. The sources area discussed here is wide, over 2 million km² according to the wave model, and the associated Rayleigh waves are recorded at land stations located several thousands of kilometers away, as in the case of body-waves. Our integrated analysis also illustrates the complex relation that links storms to microseismic sources in terms of location

and intensity, and also indicates that in some cases microseisms cannot be treated as punctual and stagnant sources. These conclusions call for more caution when using seismic noise as constraints for seismic tomography or for indirect observation of storminess. Nevertheless, the wave model proves to be able to capture most of this complexity. Therefore, by providing indication on where and when to look for microseismic sources, and on how these sources are related to storms, databases of wave-induced pressure (<http://tinyurl.com/yetsofy>) have great potential to improve the accuracy and reach of seismic noise-based analysis, such as climate studies and seismic imaging.

[11] **Acknowledgments.** This work was supported by the European Research Council (IOWAGA project) the National Ocean Partnership Program, and the Consolider-Ingenio (Topo-Iberia). We thank the operators of GEOSCOPE, Berkeley Digital Seismic Network, and IRIS/IDA for providing excellent broadband seismic data. Data were obtained from both GEOSCOPE and IRIS data centers. The U.S. National Data Buoy Center and the Coastal Data Information Program provided Wave buoy data. We also thank two anonymous reviewers for their constructive comments.

[12] The Editor thanks two anonymous reviewers for assisting with the evaluation of this paper.

References

- Algué, J. (1900), Relation entre quelques mouvements microséismiques et l'existence, la position et la distance des cyclones à Manille (Philippines), in *Congrès International de Météorologie*, pp. 131–136, Gauthier-Villars, Paris.
- Ardhuin, F., et al. (2010), Semi-empirical dissipation source functions for ocean waves. Part I: Definition, calibration, and validation, *J. Phys. Oceanogr.*, *40*, 1917–1941, doi:10.1175/2010JPO4324.1.
- Ardhuin, F., E. Stutzmann, M. Schimmel, and A. Mangeney (2011), Ocean wave sources of seismic noise, *J. Geophys. Res.*, *116*, C09004, doi:10.1029/2011JC006952.
- Aster, R., D. McNamara, and P. Bromirski (2008), Multidecadal climate induced variability in microseisms, *Seismol. Res. Lett.*, *79*, 194–202, doi:10.1785/gssrl.79.2.194.
- Bernard, P. (1981), Sur l'existence et l'amplitude de la variation undécennale des microséismes météorologiques, *C. R. Acad. Sci. Paris*, *293*, 687–689.
- Bernard, P. (1990), Historical sketch of microseisms from past to future, *Phys. Earth Planet. Inter.*, *63*, 145–150, doi:10.1016/0031-9201(90)90013-N.
- Brenguier, F., N. Shapiro, M. Campillo, V. Ferrazzini, Z. Duputel, O. Coutant, and A. Nercessian (2008), Toward forecasting volcanic eruption using seismic noise, *Nat. Geosci.*, *1*, 126–130, doi:10.1038/ngeo104.
- Bromirski, P. (2009), Earth vibrations, *Science*, *324*, 1026–1027, doi:10.1126/science.1171839.
- Bromirski, P., R. Flick, and N. Graham (1999), Ocean wave height determined from inland seismometer data: Implications for investigating wave climate changes in the NE Pacific, *J. Geophys. Res.*, *104*, 20,753–20,766, doi:10.1029/1999JC900156.
- Cessaro, R. K. (1994), Sources of primary and secondary microseisms, *Bull. Seismol. Soc. Am.*, *84*, 142–148.
- Chevrot, S., M. Sylvander, S. Benahmed, C. Ponsolles, J. M. Lefèvre, and D. Paradis (2007), Source locations of secondary microseisms in western Europe: Evidence for both coastal and pelagic sources, *J. Geophys. Res.*, *112*, B11301, doi:10.1029/2007JB005059.
- Grevenmeyer, I., R. Herber, and H.-H. Essen (2000), Microseismological evidence for a changing wave climate in the northeast Atlantic Ocean, *Nature*, *408*, 349–352, doi:10.1038/35042558.
- Hasselmann, K. (1963), A statistical analysis of the generation of microseisms, *Rev. Geophys.*, *1*, 177–210, doi:10.1029/RG001i002p00177.
- Haubrich, R. A., and K. McCamy (1969), Microseisms: Coastal and pelagic sources, *Rev. Geophys.*, *7*, 539–571, doi:10.1029/RG007i003p00539.
- Kedar, S., M. Longuet-Higgins, F. Webb, N. Graham, R. Clayton, and C. Jones (2008), The origin of deep ocean microseisms in the North Atlantic Ocean, *Proc. R. Soc. A*, *464*, 777–793, doi:10.1098/rspa.2007.0277.
- Landès, M., F. Hubans, N. Shapiro, A. Paul, and M. Campillo (2010), Origin of deep ocean microseisms by using teleseismic body waves, *J. Geophys. Res.*, *115*, B05302, doi:10.1029/2009JB006918.
- Longuet-Higgins, M. (1950), Theory of the origin of microseisms, *Philos. Trans. R. Soc. A*, *243*, 1–35, doi:10.1098/rsta.1950.0012.
- Miche, M. (1944), Mouvements ondulatoires de la mer en profondeur constante ou décroissante, *Ann. Ponts Chaussées*, *114*, 131–164.

- Schimmel, M., and J. Gallart (2004), Degree of polarization filter for frequency-dependent signal enhancement through noise suppression, *Bull. Seismol. Soc. Am.*, *94*, 1016–1035, doi:10.1785/0120030178.
- Schimmel, M., E. Stutzmann, F. Arduin, and J. Gallart (2011), Polarized Earth's ambient microseismic noise, *Geochem. Geophys. Geosyst.*, *12*, Q07014, doi:10.1029/2011GC003661.
- Schulte-Pelkum, V., P. S. Earle, and F. L. Vernon (2004), Strong directivity of ocean-generated seismic noise, *Geochem. Geophys. Geosyst.*, *5*, Q03004, doi:10.1029/2003GC000520.
- Shapiro, N., M. Campillo, L. Stehly, and M. H. Ritzwoller (2005), High-resolution surface-wave tomography from ambient seismic noise, *Science*, *307*, 1615–1618, doi:10.1126/science.1108339.
- Stutzmann, E., M. Schimmel, G. Patau, and A. Maggi (2009), Global climate imprint on seismic noise, *Geochem. Geophys. Geosyst.*, *10*, Q11004, doi:10.1029/2009GC002619.
- Tolman, H. L. (2008), A mosaic approach to wind wave modeling, *Ocean Modell.*, *25*, 35–47, doi:10.1016/j.ocemod.2008.06.005.
- Tsai, V. C. (2009), On establishing the accuracy of noise tomography traveltime measurements in a realistic medium, *Geophys. J. Int.*, *178*, 1555–1564, doi:10.1111/j.1365-246X.2009.04239.x.
- Zhang, J., P. Gerstoft, and P. Shearer (2010a), Resolving P-wave travel-time anomalies using seismic array observations of oceanic storms, *Earth Planet. Sci. Lett.*, *292*, 419–427, doi:10.1016/j.epsl.2010.02.014.
- Zhang, J., P. Gerstoft, and P. D. Bromirski (2010b), Pelagic and coastal sources of P-wave microseisms: Generation under tropical cyclones, *Geophys. Res. Lett.*, *37*, L15301, doi:10.1029/2010GL044288.